Structure of Model Waxes: Conformational Disorder and Chain Packing in Crystalline Multicomponent *n*-Alkane Solid Solutions

D. Clavell-Grunbaum, H. L. Strauss, and R. G. Snyder*

Department of Chemistry, University of California, Berkeley, California 94720-1460

Received: August 23, 1996; In Final Form: November 1, 1996[⊗]

The interlamellar disorder in waxes is a major factor in determining their unique physical properties. We have measured by Raman and infrared spectroscopies the conformational disorder and chain packing in the interlamellar region of a number of model *n*-alkane waxes consisting of 2, 3, and 4 components with chain lengths in the range from 20 to 40 carbons. Most of the mixtures studied have a constant chain length difference of four carbons between their components, in which case they are crystalline solid solutions with lamellar structures similar to pure *n*-alkanes with orthorhombic subcells. Chain packing density is lower in the interfacial region due to the chain length mismatch. Void volume and lamellar surface roughness are reduced by the formation of gauche bonds near the chain ends and through longitudinal displacement of the chains, so that the interfacial packing resembles that found in the high-temperature hexagonal phase of pure *n*-alkanes. The relative degree of disordering is highly sensitive to the chain length difference but is rather insensitive to the number of components or their average chain length. We also report on (i) the distribution of disorder among the individual components, (ii) the concentration of disorder for the orthorhombic (room temperature) and hexagonal (high temperature) phases, as measured by specific conformational sequences, and (iii) the temperature dependence of disorder for the individual components of a three-component mixture as it is warmed.

I. Introduction

Naturally occurring lipid assemblies, such as biomembranes and waxes, are complex mixtures with properties largely determined by the polymethylene chains that dominate the composition. Simple mixtures of *n*-alkanes or their derivatives tend to mimic the properties and behavior of natural assemblies and are therefore frequently used as model systems for molecular-level investigation. However, nearly all the studies of this type have focused on binary mixtures. Diffraction techniques have usually been employed to determine structure because they are highly sensitive to crystal order: Wide-angle reflections provide precise lateral unit-cell dimensions and reveal the type of lateral chain packing, while lamellar reflections can indicate, among other things, whether a mixture is a solid solution or is phase separated.

Most studies have been on model *n*-alkane mixtures with chain lengths in the range 20−26 carbons and chain length differences from one to two carbons.[1−4] Sirota and co-workers[5] have determined the crystal structures of a number of binary mixtures in the hexagonal phase. Using electron diffraction, Dorset[6−9] has studied a wide range of binary mixtures and in some cases has observed spontaneous microphase separation, a phenomenon first noted by Mazee.[10] Dorset[11] has also recently reported an electron diffraction study of waxes. Phase transitions in *n*-alkanes and petroleum-related waxes have recently been reviewed by Srivastava et al.[12]

In the present work, we focus on conformational disorder. Such disorder, which lies in the interlamellar region, is inherent to *n*-alkane mixtures and imparts to them their waxlike properties. This aspect has rarely been studied mainly for lack of suitable methods. We have adapted for this purpose infrared and Raman spectroscopies, which are sensitive to both conformational disorder and crystal structure. Raman spectroscopy can be used to measure the total disorder and its distribution among the various *n*-alkane components. Infrared spectroscopy can be used to identify specific conformational sequences and to measure their concentration.

The *n*-alkane mixtures studied here have 2, 3, and 4 components whose chain length difference is usually kept constant at four carbons. These mixtures are solid solutions, although they may undergo some slight demixing. For simplicity, we have considered only equimolar mixtures.

Previous vibrational spectroscopic studies on conformational disorder in *n*-alkane mixtures are few in number. The most extensive is that on C_{19}/C_{21}, in which chain end disorder was determined by an infrared CD_2 substitution method.[13] The conformation of the penultimate CC bonds in this mixture was determined as a function of concentration and temperature. In a separate study we used Raman spectroscopy to measure conformational disorder in the C_{46}/C_{50} mixture as a function of concentration.[14]

II. Experimental Procedures

A. Samples and Mixtures. The sources and manufacturers' estimate of purity of the *n*-alkanes (n-C_nH_{2n+2}) used are as follows: $n = 20$, 22, 24, 26, 28, 30, 32, 36 (described in ref 15, purity >99.8%); $n = 31$ (TCI, purity unknown); $n = 33$, 34, 40 (Aldrich, purity 98%); $n = 38$ (Fluka Chemie AG, purity >98%).

The following equimolar mixtures were studied. Binary: 30/31, 30/32, 30/33, 30/34, 30/36, 30/38, 30/40; 24/28, 28/32, 32/36, 34/38, 36/40; tertiary: 20/24/28, 24/28/32, 28/32/36, 30/34/38, 32/36/40; quaternary: 24/28/32/36. Solid solutions were prepared by melting together equimolar amounts of the components. After thorough mixing, the melt was cooled to room temperature within 3 min.

B. Measurement of Raman Spectra. Raman spectra were measured with a Spex Model 1403 double monochromator controlled by a Spex Datamate DM1B computer. The incident radiation was the 514.5 nm argon laser line. The scattered

* To whom correspondence should be addressed.

[⊗] Abstract published in *Advance ACS Abstracts,* December 15, 1996.

S1089-5647(96)02616-8 CCC: $14.00

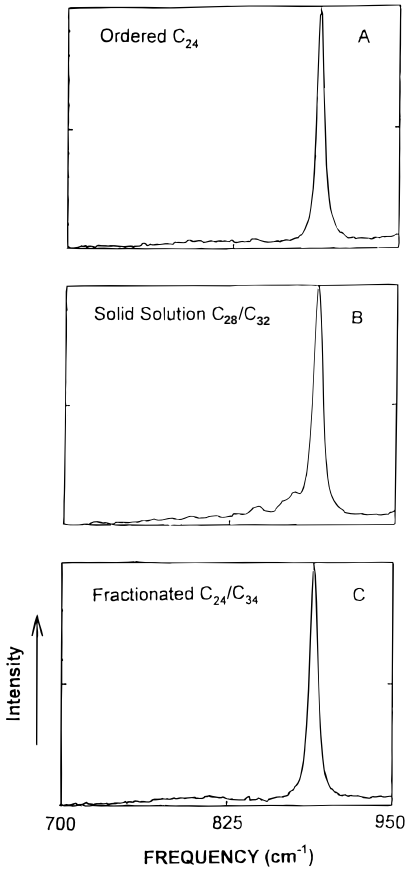

Figure 1. Raman spectra of pure crystalline C_{24} and the melt-crystallized binary mixtures 1:1 C_{28}/C_{32} and C_{24}/C_{34} at room temperature, illustrating the sensitivity of the 700−900 cm^{-1} region to conformational disorder.

radiation was passed through a polarization scrambler at the entrance slit. The resolution was 4 cm^{-1} at frequencies above 700 cm^{-1} and 2 cm^{-1} below.

The samples were held in open-ended Pyrex capillaries. The sample surface, accessible at the open end, was exposed directly to the incident laser radiation. The temperature of the sample was controlled to within 1 °C with the thermostating arrangement described in ref 16.

III. Methods for Measuring of Conformational Disorder

A. Total Disorder. Total conformational disorder was estimated from the integrated intensity of a taillike feature in the Raman spectrum that extends from the low-frequency side of the intense band at 890 cm^{-1}. This tail, which consists of a multitude of overlapping bands originating from chains with conformationally disordered ends, will be referred to as the "800 cm^{-1} tail". Its contour is generally smooth except for the presence of bands near 870 and 845 cm^{-1}. These represent the specific chain end conformational sequences egt and etg, respectively. (We will use t and g to indicate trans and gauche CC bonds and e to indicate terminal CC bonds.) The use of these bands in analyzing conformational disorder is discussed in ref 14. The intense band at 890 cm^{-1} will be used as an internal reference, since it is a measure of chains with ordered ends or, more precisely, chain ends that terminate in a sequence of six or more trans bonds.[16]

Figure 1 illustrates qualitatively how the 800 cm^{-1} tail relates to conformational disorder. This feature is not discernible in the spectrum (A) of pure C_{24}, which is highly ordered. Nor is it discernible in the spectrum (C) of 1:1 C_{24}/C_{34}, because the large chain length difference for this mixture results in a high degree of phase separation, producing ordered phases of almost pure *n*-alkanes. For 1:1 C_{28}/C_{32}, however, the 800 cm^{-1} tail is present (spectrum B), since this mixture is a solid solution and is therefore disordered.

TABLE 1: Frequencies and Widths of the Raman LAM-3 Band for Crystalline *n*-Alkanes (C_n) at Room Temperature

n	freq, cm^{-1}	width,[a] cm^{-1}	n	freq, cm^{-1}	width,[a] cm^{-1}
20	324.9	8.2	32	213.3	6.5
22	303	12.4	33	206.9	6.6
24	280.1	5.8	34	200.7	8.3
26	261	7.1	36	191.6	8.5
28	242.3	4.9	38	180.8	7.7
30	226.4	5.6	40	172.3	7.2
31	219.7	6.2			

[a] Fwhm width measured with a resolution of 2 cm^{-1}.

A weak broad band centered near 800 cm^{-1} was sometimes observed even for ordered samples. This band, which appears weakly in Figure 1C, is from the Pyrex sample holder. Normally it can be ignored.

The concentration of disorder is assumed proportional to $R^{\mathrm{Ram}}{}_{800}$, which is the normalized intensity of the 800 cm^{-1} tail defined as

$$R^{\mathrm{Ram}}{}_{800} = I_{800}/(I_{890} + I_{800}) \quad (1)$$

This quantity measures disorder if the mixture consists of only two fractions, one highly ordered and one highly disordered. To a good approximation, this is the case since the spectrum of a crystalline mixture can be separated into a spectrum of a crystalline component with all-trans chains packed in an orthorhombic subcell and a spectrum of a phase that resembles, but is not exactly identical to, the spectrum of a liquid *n*-alkane.

B. Disorder for the Individual Components. *1. LAM-3 Widths.* The distribution of conformational disorder among the components of a mixture can be estimated from the increase in the widths of their LAM-3 Raman bands in going from pure *n*-alkanes to *n*-alkanes in the mixtures. These low-frequency, relatively intense bands represent the third-order member of the longitudinal acoustic modes (LAM) progression.[17] The frequency of LAM-3 is highly dependent on (approximately inversely proportional to) chain length (Table 1). Therefore, the LAM-3 bands, and hence the individual *n*-alkanes, can be distinguished. Both the width and frequency of this band are sensitive to chain end disorder. (While the LAM-1 band is considerably more intense than LAM-3,[17] it is not used to measure disorder because, as discussed in ref 18, its frequency is 3 times less sensitive to chain length than for LAM-3.)

The response of the width of LAM-3 to changes in conformational disorder is illustrated in Figure 2 for the *n*-alkane C_{32} in a number of different systems. As expected, the LAM-3 band of C_{32} is narrowest for pure C_{32} (spectrum A). It broadens significantly in going to the 1:1 solid solution C_{28}/C_{32}, in which C_{32} is more disordered (spectrum B). The LAM-3 width for C_{32} in the mixture 1:1:1 $C_{28}/C_{32}/C_{36}$ (spectrum C)—also a solid solution—is similar to that for C_{28}/C_{32}.

The chain end disorder associated with a given *n*-alkane in a mixture is assumed proportional to the increase in the LAM-3 width in going from the pure *n*-alkane to the same *n*-alkane in the mixture. The width increase is defined

$$\Delta W_{1/2} = [\Delta\nu_{1/2}(\mathrm{mix}) - \Delta\nu_{1/2}(\mathrm{pure})]/\Delta\nu_{1/2}(\mathrm{pure}) \quad (2)$$

where $\Delta\nu_{1/2}$ is the half-width, which we will express as full width at half-maximum (fwhm).

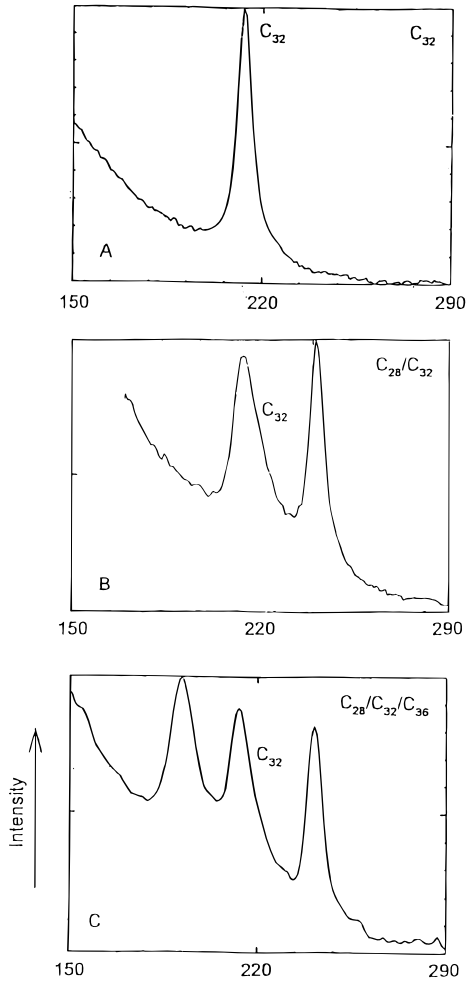

Figure 2. Room temperature Raman spectra of pure crystalline C_{32} and the mixtures 1:1 C_{28}/C_{32} and 1:1:1 $C_{28}/C_{32}/C_{36}$ in the low-frequency region, illustrating how the LAM-3 bandwidth of C_{32} changes with conformational disorder.

2. LAM-3 Widths for Pure n-Alkanes. We found that the widths of the LAM-3 bands for pure n-alkanes at room temperature are dependent on chain length. This dependence was unexpected but not a serious complication. We will digress somewhat to offer an explanation for this phenomenon. A plot of width versus chain length is not monotonic: It shows maxima at C_{22} and C_{36} (Figure 3). We believe the variation with chain length results from intrachain interaction between the LAM-3 vibration and some nearby TAM-k' (transverse acoustic mode, order k') vibration. These latter type of modes, which involve CCC bending internal coordinates,[19,20] have Raman intensities that are negligible relative to those of the LAM-k (k odd) bands. Maximal LAM-3/TAM-k' interaction occurs when LAM-3 and TAM-k' have the same frequency and when k' of TAM-k' is a multiple of 3 so as to match the symmetry of LAM-3. If these conditions are satisfied, the normal coordinates of LAM-k and TAM-k' will mix, and TAM-k' will take on one-half the intensity of LAM-3. Since the interaction causes the bands to move slightly apart, LAM-3 will appear to broaden. Broadening will also occur if the frequencies of LAM-3 and TAM-k' are not exactly the same.

The situation for C_{22}, whose LAM-3 bandwidth corresponds to the first maximum in Figure 3, is depicted in Figure 4, which shows the dispersion curve associated with the LAM and TAM modes of an *all-trans*-polymethylene chain.[21] The LAM-3 and TAM-9 modes of C_{22} have nearly the same frequency; TAM-9 has the correct symmetry. The other symmetry-eligible TAM modes ($k' = 6$ and 12) are too far removed in frequency to interact. Figure 4 predicts that the next *n*-alkane for which there will be a resonance between LAM-3 and TAM-k' will have a chain length between 34 and 38 carbons and that the interaction will be with TAM-12. Indeed, Figure 3 shows that the next maximum (that is, the next resonance) actually occurs at $n = 36$, in good agreement with the predicted value.

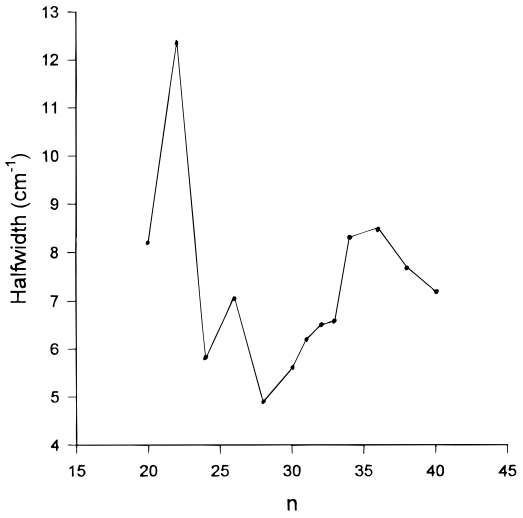

Figure 3. Raman LAM-3 band widths (fwhm) for pure crystalline *n*-alkanes at room temperature plotted against chain length (n = number of carbons).

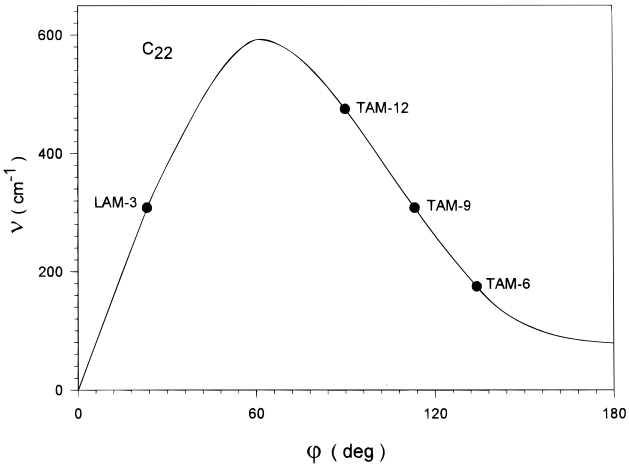

Figure 4. Approximate locations of the LAM-3 and TAM-k (k = 6, 9, 12) modes of C_{22} with respect to the *trans*-polymethylene chain dispersion curve associated with these modes. The frequencies of LAM-3 and TAM-9 for C_{22} are nearly the same, which allows them to mix. This is not the case for C_{20} and C_{24}.

The broadening mechanism proposed is confirmed through a calculation of the isotropic Raman spectra of the all-trans *n*-alkanes C_{20}, C_{22}, and C_{24}. The variations in the shapes of the LAM-3 bands observed for this series can be nicely accounted for as a result of intrachain resonance.[22] The calculated spectra are shown in Figure 5. A strong LAM-3/TAM-9 interaction occurs for C_{22}, causing LAM-3 to be split into two components of nearly equal intensity. This does not happen for C_{20} or C_{24}. The results of these calculations are in excellent agreement with observation. (The parameters we used to calculate the spectra were determined earlier from the isotropic Raman spectra of liquid *n*-alkanes.[23,24])

3. LAM-3 Widths for End-Disordered n-Alkanes. Conformational disorder introduced randomly at, or near, the ends of chains that are otherwise all-trans causes (i) the LAM-3 band

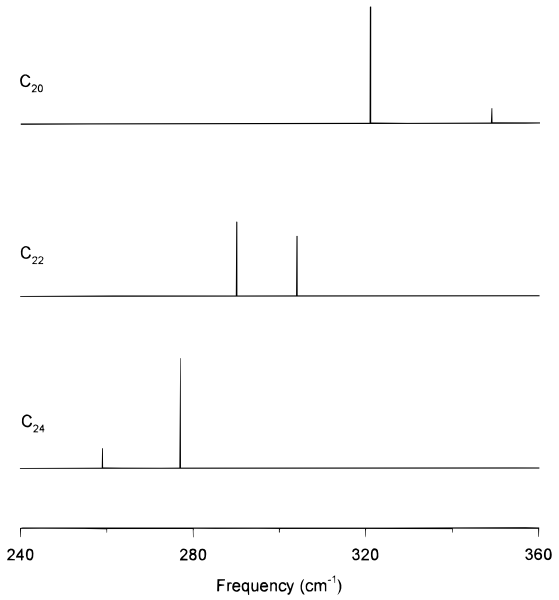

Figure 5. Calculated Raman spectra of all-trans C_{20}, C_{22}, and C_{24} in the LAM-3 band region. For C_{22} there is a strong interaction between the LAM-3 and TAM-9 modes which causes the LAM-3 band to split.

of an assembly of such chains to broaden relative to the LAM-3 band of the all-trans chain and (ii) the peak frequency to shift upward (Figure 2). The latter results from an increase in intensity on the high-frequency side of the LAM-3 band originating from the chains with disordered ends. The disordered chains have higher LAM-3 frequencies because their lengths are in effect shorter than those of the corresponding all-trans form.[18]

Simulated spectra are again helpful. The response of the LAM-3 bands to chain end disorder was explored by calculating the isotropic Raman spectra of an ensemble of chains with randomly disordered ends.[22] The ensemble consisted of C_{36} chains that were all-trans except for the four CH_2-CH_2 bonds nearest the ends. These latter bonds were randomly assigned trans or gauche conformations in accordance with the statistics of the liquid; that is, the interfacial region was assumed to be liquidlike. The chain-end conformational sequences were generated using the rotational isomeric state model.[25]

The spectra calculated in this way display LAM-3-like bands whose frequencies are about 10 cm^{-1} higher than the LAM-3 band of the all-trans chain. The calculated shift is near the 11 cm^{-1} shift observed for the LAM-3 band of the disordered C_{36} chains in 1:1 C_{30}^H/C_{36}^D.[18]

It is important to note that, while the calculated spectrum is sensitive to the total number of gauche bonds, it is not very sensitive to their distribution. Broadening of the LAM-3 band would thus appear to be a valid measure of total disorder. We note our results may be affected to some extent by the effect of conformational disorder on the broadening from the LAM-3/TAM-k' resonance discussed above.

IV. Dependence of Disorder on the Chain-Length Difference for Binary Mixtures

A. Results. This dependence was measured for a series of equimolar $C_{30}^H/C_{n'}^H$ mixtures ($n' = 30-34$, 36, 38, or 40). The time elapsed between the quench and the start of the Raman measurements was normally 1−2 h. It took approximately 2−3 h to determine the Raman spectrum.

Relative disorder in units of R_{800}^{Ram} is plotted as a function of chain length difference ($\Delta n = n' - 30$) in Figure 6. While the disorder is least for pure C_{30} ($\Delta n = 0$) as expected, it is not

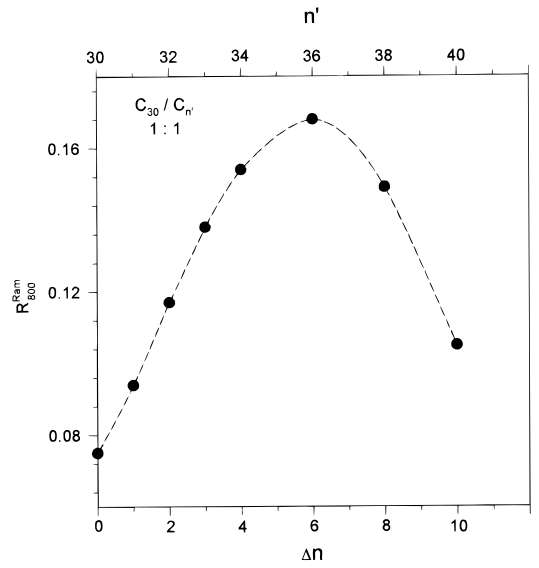

Figure 6. Room temperature conformational disorder for the 1:1 binary mixtures $C_{30}/C_{n'}$ ($n' = 30$, 31−34, 36, 38, 40) plotted against Δn, the chain length difference between the components. The measurements were completed 3−5 h after the samples were quenched.

zero. This suggests the presence of inherent disorder not associated with chain ends. In an earlier infrared study on the temperature dependence of conformational disorder in pure *n*-alkanes,[26] we found significant, roughly constant disorder at room temperature for *n*-alkanes with lengths between 20 and 60 carbons. This disorder, which was attributed to -gtg′- sequences, probably accounts for the spectral background. Infrared measurements, described below, support this interpretation.

The chain end disorder for this series of mixtures increases approximately linearly with the chain length difference Δn (Figure 6). The increase begins to taper off near $\Delta n = 4.4$ carbons; a disorder maximum is reached near $\Delta n = 6$.

B. Discussion. Earlier work[8,27] has established that stable or nearly stable solid-solutions are formed upon quenching, provided Δn is four carbons or less. As the chain length mismatch becomes greater, chain end packing becomes increasingly more difficult, and the stability of the mixture diminishes accordingly. The conformational disorder contributes to stability because gauche bonds allow the chains to extend laterally (that is, in directions parallel to the lamellar surface) which permits denser chain packing. As noted above, the increase in disorder levels off as Δn goes from four to six carbons, with a maximum near $\Delta n = 6$. This behavior is a result of microphase separation, which increases dramatically as the chain length difference exceeds four carbons.[27] Disorder decreases with increased demixing because the surface of the domains, which are dominated by one component, tend to be highly ordered.

For $\Delta n \geq 4$, the demixing may be spontaneous, that is, occur in real time. As a result, the disorder/chain length plot can be time dependent. For example, the plot shown in Figure 6 is based on measurements that were completed from 3 to 5 h after the quench. Because of the spontaneous demixing known to occur for some of these mixtures, a shorter interval would shift the maximum toward larger Δn and increase the amount of disorder in the $\Delta n = 6$ region.

The relative stabilities of $C_{30}^H/C_{n'}^H$ mixtures have been determined by electron diffraction measurements.[28] It is informative to relate the stability determined in this way to the degree of conformational disorder determined spectroscopically. One diffraction-determined point of reference is the value of Δn that defines the sharp boundary between solid solutions that are indefinitely stable and those that are metastable. (From the

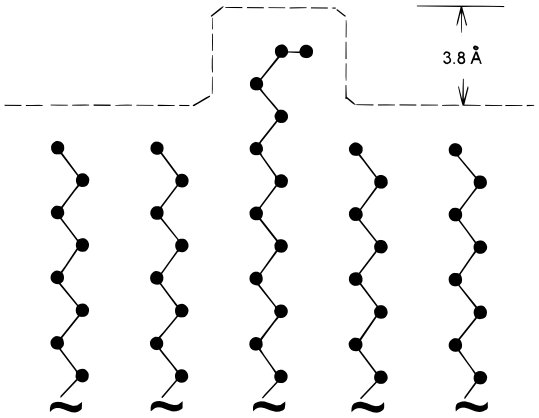

Figure 7. Minimum protrusion length needed to form the simplest fold—one in which the penultimate CC bond is gauche.

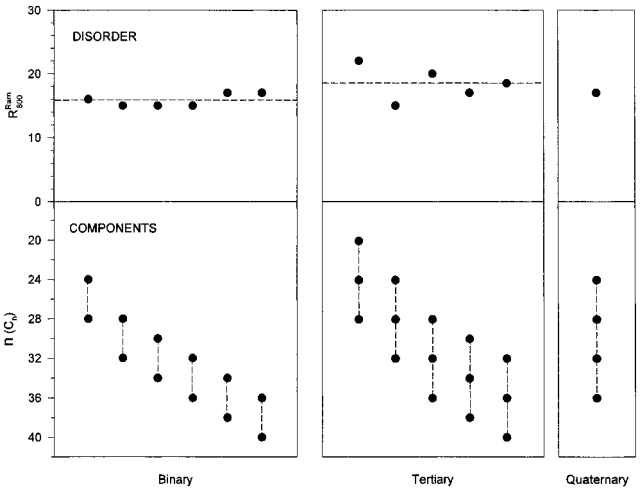

Figure 8. Total conformational disorder (in units of R^{Ram}_{800}) associated with equimolar binary, tertiary, and quaternary *n*-alkane mixtures at room temperature. The components of the mixtures are indicated.

electron diffraction point of view, a solid solution is metastable if superlattice-like reflections appear in the diffraction pattern of the mixture. Whether or not these reflections appear is a sensitive function of Δn.[6]) The value of Δn at the boundary is 4.4 ± 0.1 carbons ($n' = 34.4$).[28] This is very near the spectroscopically determined value of 4.2 ± 0.2 that marks the onset of demixing. (The onset value of Δn is the value of Δn at which nonlinearity first becomes apparent in the disorder vs Δn plot (Figure 6).) In short, demixing and metastability commence at the same value of Δn.

A second reference is the electron diffraction determined value of Δn that defines the boundary between the metastable solid solution and the fractionated solid. (In a fractionated solid, the components are nearly completely separated.) As Δn increases, the onset for the fractionation is signaled by the appearance of reflections that correspond to the lamellar spacings of the pure *n*-alkanes. We find that the values of Δn for the onset of fractionation[28] and for maximum conformational disorder (Figure 6) are nearly identical, both 6.0 ± 0.3.

We now consider an aspect of the disorder/chain length difference plot in Figure 6 that is structurally revealing. It is the existence of significant chain-end conformational disorder in those mixtures in which the chain length difference per se is too small to allow chain end folding. For a chain to fold over, it must extend a minimum of four carbons above the surface defined by the neighboring chains. This is illustrated in Figure 7, which shows that, if $\Delta n = 4$, the only fold possible is one in which the penultimate CC bond assumes a gauche conformation. (In this figure, the chain surfaces are defined using van der Waals radii; the distances between nearest-neighbor chains are those for orthorhombic packing. For simplicity, the chains are placed in a common plane.) Thus, if the chains in a binary mixture are all-trans and are disposed symmetrically about the layer midplane defined by the chain centers, Δn must be greater than 6 for folding. Such a highly symmetrical arrangement is, of course, unlikely. However, even the most asymmetric disposition of chains would still require $\Delta n > 3$ for folding.

Our measurements show that disorder increases smoothly as Δn goes from 0 to 4 carbons. This indicates that the chains, in order to minimize interlamellar voids, undergo a significant degree of longitudinal translation. Displacements of this sort have the effect of increasing the average protrusion length and thus account for folding when Δn is less than four carbons. The absence of an abrupt increase in disorder as Δn goes from three (folding not allowed) to four (folding allowed) would also be explained. Total disorder would nevertheless still be determined by the chain length difference.

In this way the structure of the mixture in the interfacial region resembles that for the high-temperature hexagonal phase of a pure *n*-alkane, which phase is characterized by longitudinally displaced chains.[29] Infrared measurements, to be described below in section VIII.A, also indicate similarities between the orthorhombic mixtures and the hexagonal *n*-alkanes. One such similarity is that the concentration of disorder for the room-temperature mixtures is about two-thirds that of the hexagonal phase.

Another feature of interest in Figure 6 is the surprisingly high degree of disorder found in binary mixtures with chain length differences large enough to ensure essentially complete phase separation. Nearly pure *n*-alkane phases should result[8] so that very little conformational disorder is expected. An example is the 1:1 C_{30}/C_{40} mixture, which is disordered to approximately the same extent as the solid solution C_{30}/C_{32} (Figure 6).

A possible explanation is that the disorder is "frozen in" during the quench. Room-temperature stability for such a system seems possible judging from the onset temperatures for longitudinal diffusion that have been estimated from studies on nematic-like *n*-alkanes[30] and long *n*-alkane mixtures.[31] A related explanation would be that the components of room-temperature C_{30}/C_{40} are not entirely separated.

V. Total Disorder in Multicomponent Mixtures

Total conformational disorder at room temperature has been determined for eight binary, five tertiary, and one quaternary equimolar mixtures whose components are such that they can be ordered as $C_n/C_{n+4}/C_{n+8}/...$ The choice of a chain length difference of four carbons is a compromise. From the spectral standpoint, large chain length differences are desirable to keep the LAM-3 bands associated with different *n*-alkanes as far apart in frequency as possible. On the other hand, larger chain length differences increase phase separation, which we wish to minimize. The compromise value, $\Delta n = 4$, permits the LAM-3 bands to be resolved, albeit sometimes with difficulty, and leads to solid solutions that at most are only slightly demixed.

Relative disorder per chain was estimated, as discussed earlier, from the intensity of the 800 cm^{-1} tail in the Raman spectrum. As shown in Figure 8, the disorder in these mixtures is constant to within about 20% and is therefore nearly independent of the number of components and the average chain length.

VI. Distribution of Disorder among the Components

A. Binary Mixtures. The distribution of disorder for the binary solid solutions C_n/C_{n+4} ($n = 24$, 28, 30, 32, 34, or 36),

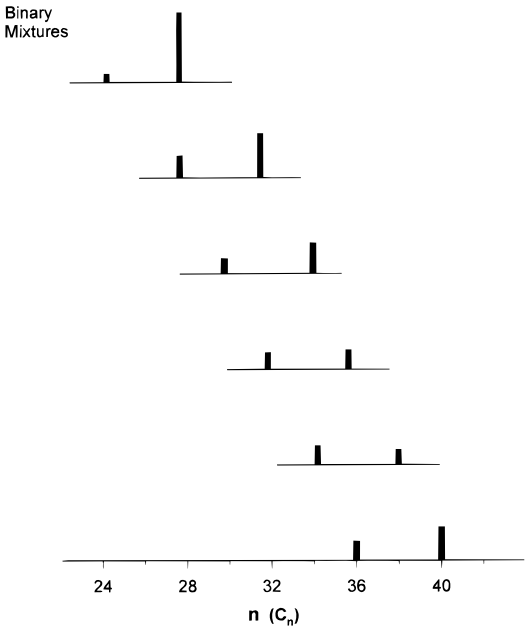

Figure 9. Bar graphs indicating the distribution of conformational disorder among the components of 1:1 binary *n*-alkane mixtures at room temperature. The disorder is measured by the normalized broadening ($\Delta W_{1/2}$) of the Raman LAM-3 bands, that is, by $\Delta W_{1/2}$ defined by eq 2. The bar heights are proportional to $\Delta W_{1/2}$. The scale is the same for all mixtures in this figure and Figure 10 to allow cross comparison.

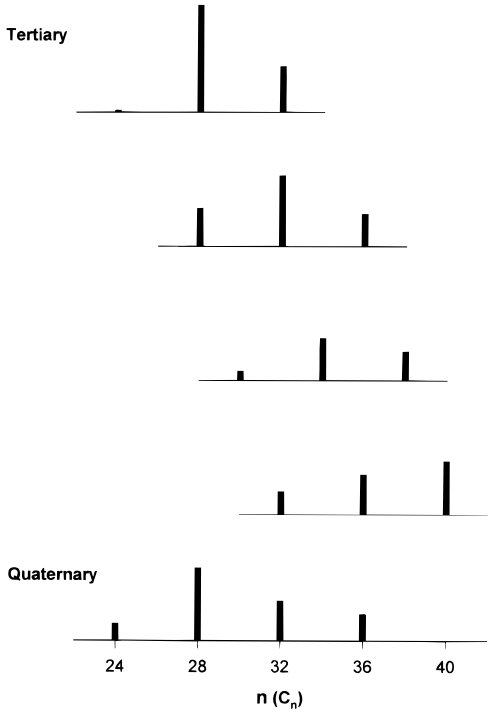

Figure 10. Distribution of conformational disorder among the individual components of equimolar tertiary and quaternary *n*-alkane mixtures at room temperature. (See caption for Figure 9.)

which was estimated from the normalized broadening of the Raman LAM-3 band (eq 2), is displayed in Figure 9. A common scale is used so that different mixtures can be compared.

The longer chains in these binary mixtures are generally more disordered than the shorter ones. This finding is in accord with our earlier measurements on the C_{19}/C_{21}[13] and C_{30}/C_{36}[18] and with expectations based on simple chain-packing models. However, the present measurements reveal that, with increasing average chain length, the concentration of disorder for the long and short chains becomes more nearly equal. Specifically, the disorder ratio—long chain to short chain—is about 8 for the relatively short chain mixture C_{24}/C_{28}. This ratio is similarly large, about 6.7, for the orthorhombic short chain mixture C_{19}/C_{21} at 275 K.[13] In contrast, the longer chain pairs, C_{32}/C_{36}, C_{34}/C_{38}, and C_{36}/C_{40}, have much lower values, averaging 1.4 $\pm$ 0.5. The lower values may be a consequence of the diminished importance of the chain length difference due to the increase in the average chain length, in which case the longitudinal displacement of the long and short chains may become more equal so that the disorder is more equally distributed.

B. Three- and Four-Component Mixtures. An intriguing question, one critical to understanding complex mixtures, is how the *n*-alkanes in a three-component mixture distribute themselves. The longest and shortest alkanes in the three-component mixtures considered here differ in length by eight carbons. A binary mixture with an eight-carbon chain length difference would certainly phase separate. However, phase separation of the corresponding pair of components (C_n and C_{n+8}) in the 3-component mixture will be modulated by the intermediate component, C_{n+4}. An interesting aspect of this concerns the compromising role that the middle component must play in trying to mix with two sets of chains with contrary needs for optimum packing—the chains of one set being 4 carbons shorter and those of the other being four carbons longer. We would not therefore expect the miscibility exhibited by the three-component mixture to match that of the corresponding (Δn = 4) binary mixture.

A significant difference found between the two- and three-component mixtures is in the distribution of disorder among the components (Figure 10). In the binary mixtures, the longest *n*-alkane is known to be the most disordered. For the tertiary mixtures, it is the middle chain. This suggests the longest chains may be more aggregated than those in the binary mixtures, since aggregation would reduce the conformational disorder of this component. Measurements on demixing in $C_{28}/C_{32}/C_{36}$ are currently being carried out using the infrared isotope method.[32] Preliminary results indicate that both the longest and the shortest chains are somewhat aggregated, while the intermediate chain remains randomly dispersed.[27]

For the one quaternary mixture, $C_{24}/C_{28}/C_{32}/C_{36}$, we considered, the next-to-shortest chain appears to be the most disordered component.

VII. Temperature Dependence of Disorder for a Three-Component Mixture

Relative changes in conformational disorder for each component in the mixture $C_{28}/C_{32}/C_{36}$ were determined as the sample was warmed from room temperature to about 60 °C, which is near the onset of melting. To monitor these changes, we used the frequencies of the Raman LAM-3 bands, rather than their widths. (Increasing frequency indicates increasing disorder, as discussed in section III.B.3. Frequency/temperature plots are displayed in Figure 11. The relative concentrations of disorder for each component at room temperature are indicated in Figure 10.)

Each component responds differently to warming. With increasing temperature, the longest chain (C_{36}) disorders much more than either C_{28} or C_{32}. We note that the shortest chain (C_{28}), which disorders least, behaves in an anomalous manner between 30 and 50 °C. Beginning at about 30 °C, the LAM-3 band decreases in frequency instead of increasing as it does for the other components. A minimum frequency is reached near

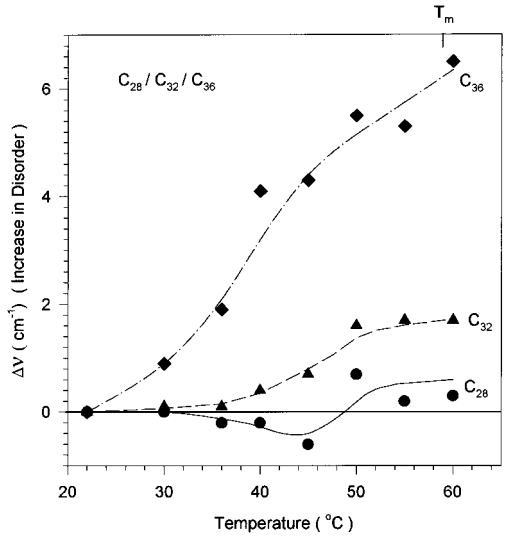

Figure 11. Changes in conformational disorder as a function of temperature for the components of the 1:1:1 $C_{28}/C_{32}/C_{36}$ mixture. The changes were monitored on the basis of the frequency shift ($\Delta\nu$) of LAM-3 from its room temperature value $\Delta\nu = \nu(T) - \nu(\mathrm{RT})$.

45 °C. It would then appear that initial warming causes C_{28} to become slightly more ordered. The disorder/temperature plot for the chain of intermediate length parallels that for C_{28}. Breaks for both C_{28} and C_{32} occur near 50 °C, which are probably associated with the transition to the hexagonal phase that is indicated in the DSC (differential scanning calorimetry) curve. A more or less well-defined break for C_{36} occurs around 36 °C. This is probably associated with the dissolution of microdomains indicated by a "mixing" endotherm in the DSC.[27] The dissolution of domains results in increased chain-end disorder for the longest component. We have observed the same phenomenon, long-chain disorder accompanying domain dissolution, for C_{30}/C_{36}.[18]

VIII. Measurement of Conformational Disorder by Infrared Spectroscopy

Infrared spectra can provide additional information about conformational disorder that is more quantitative and location specific than that from Raman spectra. Our measurements are based on the methylene wagging bands found in the 1280−1400 cm^{-1} region.[16,33] The vibrations associated with these bands are more or less localized within specific conformational sequences (-gtg′- at 1306 cm^{-1}, eg- at 1341 cm^{-1}, -gg- at 1353 cm^{-1}, and -gtg- at 1366 cm^{-1}). These bands have frequently been used to analyze the conformation of polymethylene assemblies such as *n*-alkanes in their orthorhombic and hexagonal phases[16] and phospholipid bilayers in their gel and liquid crystal phases.[34] The spectrum shown in Figure 12, which is of C_{30}/C_{34} at 60.2 °C, is typical of those of our mixtures.

A. Conformation of the Penultimate CC Bond. The fraction (f_{eg}) of the penultimate CC bonds that are gauche has been estimated from the intensity of 1341 cm^{-1} band. This measure of disorder is well-defined in that it refers to a specific CC bond, one located where disorder is maximum. The value of f_{eg} was derived from, and is proportional to, R^{IR}_{1341}, which is defined

$$R^{IR}_{1341} = I_{1341}/I_{1375} \qquad (3)$$

where I_{1341} is the integrated intensity of the 1341 cm^{-1} band. The intensity (I_{1375}) of the methyl umbrella band was used as a measure of the number of chains sampled, since this band is highly localized and not much affected by disorder or physical state. The proportionality constant (K) that relates to f_{eg} to the measured quantity ($f_{eg} = KR^{IR}_{1341}$) was determined from the values of f_{eg} and R^{IR}_{1341} measured for the same *n*-alkane systems. The four estimates of K were obtained from hexagonal phase C_{21} and C_{29} (C_{29} at two temperatures[29]) and from 1:1 C_{19}/C_{21} in the orthorhombic phase.[13] In each case, the value of f_{eg} had been previously determined by the CD_2 probe method.[13,29] The values for R^{IR}_{1341} were determined in the present work. The average value of K was estimated to be 3.5 ± 0.5. The error is based on the uncertainties associated with separating the 1341 cm^{-1} band from its background.

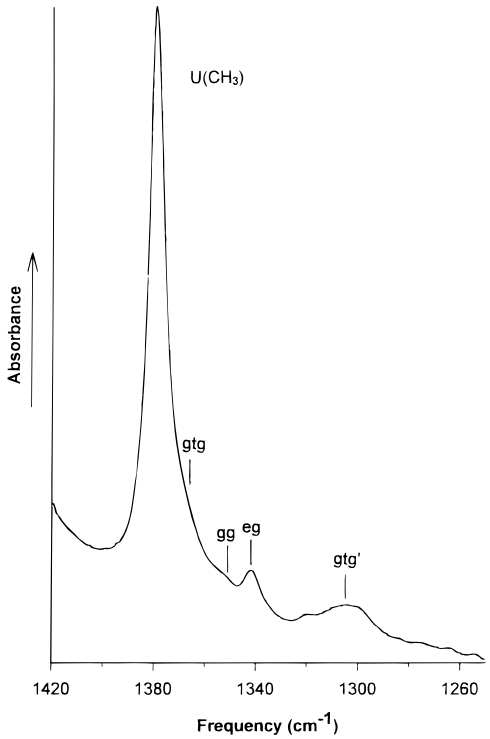

Figure 12. Infrared spectrum of 1:1 C_{30}/C_{34} at 60.2 °C in the methylene wagging mode region. The frequencies of the bands associated with specific conformational sequences are marked. (The gtg and gg bands are very weak; see text). The methyl umbrella band, which is used as an intensity reference, is marked $U(CH_3)$.

Figure 13A displays the concentrations (f_{eg}) of gauche penultimate CC bonds for selected *n*-alkanes and *n*-alkane solid solutions. The value of f_{eg} for pure *n*-alkanes at room temperature is very low (<0.2%), below the detectability limit. The values found for the room temperature mixtures are much larger—about 9.0 and 8.3% for C_{30}/C_{34} and $C_{28}/C_{32}/C_{36}$, respectively. Their near-equal value is in line with our earlier finding that disorder per chain for mixtures with a constant chain length difference of four carbons is nearly independent of the number of components. These values are about 65% of that for hexagonal phase C_{29}, underlining the similarity in the disorder between the orthorhombic mixtures and the hexagonal *n*-alkanes. Disorder for the mixtures in their hexagonal phases was also measured and found to be essentially indistinguishable from that of the hexagonal phase of the *n*-alkanes, in terms of both concentration and kinds of conformational sequences.

B. Nature of the Interlamellar Disorder. The value of f_{eg} offers a basis for estimating the extent to which the interfacial disorder is liquidlike. The value of f_{eg} for a liquid n-alkane is about 34%.[25] This value is essentially independent of chain length and temperature over the range of temperatures covered

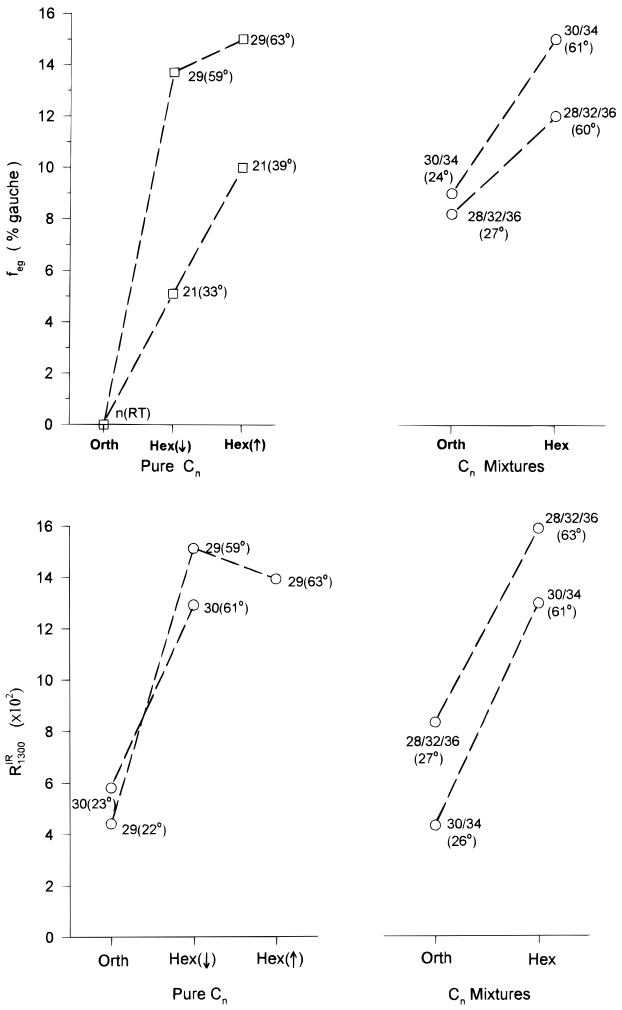

Figure 13. Disorder for selected pure and mixed n-alkanes in the orthorhombic and hexagonal phases. (HEX(↓) and HEX(↑) indicate that the hexagonal phase is near its lowest or its highest temperature limits, respectively; that is, it is just above T_α or just below T_m.) (A, top) The concentration of penultimate CC bonds that are gauche (□, determined in ref 29 using the CD_2 probe method; ○, based on the 1341 cm^{-1} infrared wagging band). (B, bottom) The relative concentration of the gtg′ sequence (based on the intensity of the 1306 cm^{-1} infrared wagging band).

in the present measurements. For comparison, f_{eg} for the orthorhombic mixtures near room temperature is about 9%. For the hexagonal mixtures near 60 °C, f_{eg} is about 14%, that is, somewhat less than half the liquid value.

The interlamellar region of the room temperature mixtures is thus much too ordered to be described as liquidlike. Comparisons based on the -gg- and -gtg- sequences lead to the same conclusion.

The low concentration of gauche bonds indicated by the infrared measurements would seem to be at odds with the Raman spectra. As we have seen, these spectra show, in addition to the band representing the egt- and etg- sequences, a broad, relatively intense band extending from about 880 to below 800 cm^{-1}. This suggests contributions to the Raman spectrum from a type of conformational disorder that is not manifest in the infrared. A sequence meeting this requirement is $et_mgt_{m'}$-. Except for eg-, this kind of sequence does not in general lead to localized modes and hence to characteristic infrared bands.[16,33] However, our calculations indicate such sequences will contribute significant intensity to the Raman spectrum over the region 700−900 cm^{-1}, that is, to the 800 cm^{-1} tail that we have used to estimate total intensity.

Lastly, we consider -gtg′- ("kink") sequences. The relative concentration of such sequences, which are represented by a band near 1300 cm^{-1}, can be estimated from the intensity ratio, $R^{IR}_{1300} = I_{1300}/I_{1375}$. Values are assembled in Figure 13B for various systems. We note that kinks seem ubiquitous to pure *n*-alkane crystals,[26] into which they are probably incorporated during crystallization. They are likely to be located in the interior of the chains.

The measured concentration of -gtg′- sequences in the two- and three-component mixtures appears to be quite different. The concentration in C_{30}/C_{34} and pure crystalline *n*-alkanes is nearly the same, indicating this sequence is not associated with the binary mixture. However, its concentration increases by a factor of 2 for $C_{28}/C_{32}/C_{36}$. The greater concentration in the three-component mixture seems reasonable in that the -gtg′- sequence needs more room than say eg- and is therefore more likely to occur in a mixture with a thicker disordered layer.

IX. Summary

The conformational disorder in a number of 2-, 3-, and 4-component equimolar *n*-alkane mixtures in the orthorhombic (room temperature) and hexagonal (high temperature) crystalline phases has been measured using Raman and infrared spectroscopies. The mixtures consist of n-alkanes with chain lengths ranging from 20 to 40 carbons. The structure of the mixtures is known to be lamellar, very similar to that of pure *n*-alkanes except for the conformational disorder in the interfacial region. At room temperature, the subcell packing is orthorhombic, becoming hexagonal at higher temperatures. The components are nearly randomly mixed if the chain length difference is less than about four carbons. Larger chain length differences lead to microphase separation, which has been considered in detail elsewhere.[8,27]

The quantitative relation between conformational disorder and the chain length difference was established for a series of binary 1:1 mixtures $C_{30}/C_{n'}$, with n' varying from 30 to 40 carbons. With an increasing chain length difference, disorder at first increases linearly. However, near $n' = 34$, the rate of increase slows as microphase separation sets in. After maximum disorder is reached near $n' = 36$, ordering occurs because the microdomains become conformationally ordered as they grow.

The components of orthorhombic mixtures with a constant chain length differences of four carbons are largely miscible. The total concentration of disorder is found to be roughly constant for all mixtures; that is, the concentration is independent of the number of components or average chain length. For binary mixtures, the longer chains are more disordered than the short ones, although the difference decreases significantly with increasing average chain length. Tertiary mixtures behave differently. Here, the chains of intermediate length are the most disordered. These chains are also more randomly distributed. The longer and shorter chains undergo some microphase separation.

The observed near-linear dependence of the concentration of conformational disorder on the chain length difference (in binary mixtures over the difference range from 0 to 4 carbons) indicates that the chains in the orthorhombic mixtures are to some extent longitudinally displaced. This displacement combined with the presence of gauche bonds helps to maximize chain-packing density in the interfacial region, which resembles that of the hexagonal phase of the *n*-alkanes.

Overall, the room temperature orthorhombic mixtures remain highly ordered. The total concentration of gauche bonds is less than 1%, which may be compared to a room temperature concentration of about 36% for *n*-alkanes in the liquid state.

The gauche concentration is of course higher in the interlamellar region, because the disorder is pretty much confined there. Thus, roughly 9% of the penultimate CC bonds are gauche—about one-fourth the value for the liquid and about two-thirds that found for crystalline *n*-alkanes in the hexagonal phase. The disorder found in the interfacial region of the room temperature mixture is, however, still relatively low, in keeping with the high degree of lamellar flatness recently reported by Dorset for waxes.[11]

As the temperature of the $C_{28}/C_{32}/C_{36}$ mixture is increased, the chain-end disorder of all the components increases, but they are affected differently. The longest chain disorders by far the most, while the shortest chain is hardly affected. The chain of intermediate length disorders somewhat more than C_{28}, but much less than C_{36}.

Acknowledgment. We gratefully acknowledge support of this work by the National Institutes of Health (Grant GM 27690). We are indebted to Dr. Douglas A. Cates for his calculations on the Raman spectra. In addition, we thank Dr. Guanghe Liang and Wenhong Yan for their help in preparing the figures.

References and Notes

(1) Luth, H.; Nyburg, S. C.; Robinson, P. M.; Scott, H. G. *Mol. Cryst. Liq. Cryst.* **1974**, *27*, 337.
(2) Gerson, A, R.; Nyburg, S. C. *Acta Crystallogr.* **1994**, *B50*, 252.
(3) Achouboudjema, Z.; Bourdet, J. B.; Petitjeau, D.; Dirand, M. *J. Mol. Struct.* **1995**, *354*, 197.
(4) Denicolo, I.; Craievich, A. F.; Doucet, J. *J. Chem. Phys.* **1984**, *80*, 6200.
(5) Sirota, E. B.; King, H. E.; Shao, H. H.; Singer, D. M. *J. Phys. Chem.* **1995**, *99*, 798.
(6) Dorset, D. L. *Macromolecules* **1985**, *18*, 2158.
(7) Dorset, D. L. *Macromolecules* **1986**, *19*, 2965.
(8) Dorset, D. L. *Macromolecules* **1990**, *23*, 623.
(9) Dorset, D. L. *Macromolecules* **1987**, *20*, 2782.
(10) Mazee, W. M. *Prepr.—Am. Chem. Soc., Div. Pet. Chem.* **1958**, *3* (4), 35.
(11) Dorset, D. L. *Acta Crystallogr.* **1995**, *B51*, 1021.
(12) Srivastava S. P.; Handoo, J.; Agrawal, K. M.; Joshi, G. C. *J. Phys. Chem. Solids* **1993**, *54*, 639.
(13) Maroncelli, M; Strauss, H. L.; Snyder, R. G. *J. Phys. Chem.* **1985**, *89*, 5260.
(14) Kim, Yesook; Strauss, H. L.; Snyder, R. G. *J. Phys. Chem.* **1989**, *93*, 485.
(15) Schaerer, A. A.; Busso, C. J.; Smith, A. E.; Skinner, L. B. *J. Am. Chem. Soc.* **1955**, *77*, 2017.
(16) Maroncelli, M; Qi, S. P.; Strauss, H. L.; Snyder, R. G. *J. Am. Chem. Soc.* **1982**, *104*, 6237.
(17) Rabolt, J. F. *CRC Crit. Rev. Solid State Mater. Sci.* **1985**, *12*, 165.
(18) Snyder, R. G.; Conti, G.; Strauss, H. L.; Dorset, D. L. *J. Phys. Chem.* **1993**, *97*, 7342.
(19) Mazur, J.; Fanconi, B. *J. Chem. Phys.* **1979**, *71*, 5069.
(20) Snyder, R. G.; Kim, Yesook *J. Phys. Chem.* **1991**, *95*, 602.
(21) Tasumi, M.; Shimanouchi, T; Miyazawa, T. *J. Mol. Spectrosc.* **1962**, *9*, 261.
(22) Cates, D. A.; Snyder, R. G. Unpublished work.
(23) Snyder, R. G. *J. Chem. Soc., Faraday Trans.* **1992**, *88*, 1823.
(24) Cates, D. A.; Strauss, H. L.; Snyder, R. G. *J. Phys. Chem.* **1994**, *98*, 4482.
(25) Flory, P. J. *Statistical Mechanics of Chain Molecules*; Wiley-Interscience: New York, 1969.
(26) Kim, Y.; Strauss, H. L.; Snyder, R. G. *J. Phys. Chem.* **1989**, *93*, 7520.
(27) Snyder, R. G.; Goh, M. C.; Srivatsavoy, V. J. P.; Strauss, H. L; Dorset, D. L. *J. Phys. Chem.* **1992**, *96*, 10008.
(28) Dorset, D. L.; Snyder R. G. *Macromolecules* **1995**, *28*, 8412.
(29) Maroncelli, M; Strauss, H. L.; Snyder, R. G. *J. Chem. Phys.* **1985**, *82*, 2811.
(30) Hagemann, H.; Strauss, H. L.; Snyder, R. G. *Macromolecules* **1987**, *20*, 2810.
(31) Zhang, W. P.; Dorset, D. L. J. *Polym. Sci., Part B., Polym. Phys.* **1990**, *28*, 1223.
(32) Snyder, R. G. Unpublished work.
(33) Snyder, R. G. *J. Chem. Phys.* **1967**, *47*, 1316.
(34) Mendelsohn, R.; Davies, M. A.; Brauner, J. W.; Schuster, H. F.; Dluhy, R. *Biochemistry* **1989**, *28*, 8934.